10

Different approaches to *ab initio* modeling of hexagonal single-wall nanotubes with large diameters

© A.V. Domnin, I.E. Mikhailov, R.A. Evarestov

Institute of Chemistry, Saint Petersburg State University,
St. Petersburg, Russia

E-mail: a.domnin@spbu.ru

Received June 26, 2024
Revised June 26, 2024
Accepted July 9, 2024

This work proposes several approaches to simplify the theoretical modeling of large diameter nanotubes. Literature analysis shows that most *ab initio* simulations of nanotubes choose small diameters to reduce computational cost. However, we show that a small torsional deformation can lead to a significant reduction in the number of atoms in the elementary cell of a chiral nanotube. We have analyzed several WS_2-based nanotubes with diameters larger than 10 nm that have been experimentally characterized. Our results were supported by density functional theory calculations. The proposed methods are suitable for modeling any nanotubes rolled up from a hexagonal layer.

Keywords: Nanotubes, *ab initio* line group theory, DFT simulations, tungsten disulfide.

DOI: 10.61011/PSS.2024.08.59064.168

1. Introduction

The hexagonal nanotubes (NT) attract attention of researches for last 30 years. Since publication of first papers of Iijima and Tenne [1,2] comprehensive theoretical and experimental studies were conducted on various types of nanotubes. The key feature of the structure of the nanotube is the presence of single direction with possible periodicity. This results in unique structural, mechanical, electronic and optical properties.

Depending on composition we can distinguish organic and inorganic nanotubes (NT). Organic NTs comprise carbon and ensembles of organic molecules. In particular, authors [3] studied structure of the organic nanotube with point symmetry C_5. The inorganic nanotubes comprise oxides or chalcogenides of transition metals, and can be also formed by atoms of boron and nitrogen [4], silicon [5] or pure metals (e.g., Ag, Pt, Fe, Co, Ni) [6]. Scope of NT application is wide, considering their medical properties [7,8], ability to adsorb gases [9], cathodoluminescence [10] and photocatalytic properties for water splitting [11].

For NT theoretical modeling it is easy to consider that nanotubes are made by rolling up from a layer. Due to symmetry limitations the nanotubes can be rolled up from the layer with rectangular, square, oblique or hexagonal lattice [12]. There are many reviews of models of „nanotube from layer", in which detail symmetry analysis is performed [13–15]. In present paper the line groups theory is used to consider NT symmetry.

Despite the development of modern computer technologies, *ab initio* modeling of nanotubes is still associated with high computational costs, especially for systems containing large number of atoms, and exactly such systems are observed in experiments. Theoretical modeling of nanotubes by *ab initio* methods not always is simple objective, especially for multiwall nanotubes. In many cases for such objectives solution we frequently use methods based on classical mechanics [16–18], but under such approach we can characterize only mechanical properties (for example, Young's modulus, Poison's ratio). The band structure is simulated using methods of quantum mechanics [13,15,19]. Besides, due to complexity of solution of the many-electron problem, it is difficult to begin *ab initio* studies of nanotubes of large diameter. Therefore, most modern papers relate to achiral nanotubes, which have higher symmetry, with diameter less than 100 Å, although experimentally obtained nanotubes are predominantly chiral and have larger diameter (10−300 nm) [20].

One of methods to solve this problem is described in paper of P.N. D'yachkov „Quantum Chemistry of Nanotubes: Electronic Cylindrical Waves" [21]. By combining the linearized connected cylindrical wave basis and the use of helical symmetry, significant success was achieved in the nanotubes modeling, however, within the framework of the used approach the modeling is carried out without geometry optimization [22], this can introduce significant error into the results.

Table 1 shows some literature data on the modeled nanotubes: their type, chirality, diameter and reference to source. For simple problems, instead of nanotubes, we can calculate the layer properties using quantum mechanics methods: the band gap, the top of the valence band, and the bottom of the conduction band [23].

In case of MD modeling of carbon nanotubes NT first of all operates as secondary system to model different processes, for example gases adsorption [9,33]. So, their diameters are limited by values below 50 Å, as during modeling in system many other molecules were involved.

Table 1. Literature data on different nanotubes studied by calculation methods

Composition	Chirality	d, Å	Method
WSSe	Armchair	35.71	DFT [24]
WS_2	Zigzag, armchair, chiral $n(2, 1)$	DFT [20] 38.48*	
WS_2	Chiral $n(4, 1)$	41.90	DFT [25]
MX (M = Ga, In; X = S, Se, Te)	Zigzag, armchair	< 80	DFT [26]
BN, TiO_2	Armchair, zigzag	29.51	DFT [27]
HfO_2, ZrO_2	Armchair, Zigzag	18.0	DFT [28]
WS_2	Armchair	32.19	DFT [10]
WS_2	Zigzag, armchair	**122.10**	DFT [11]
Si	Armchair	23.5*	MD [5]
BeO	Zigzag, armchair	< 20*	MD, DFT [18]
C	Zigzag	12.04	MD [29]
C	Zigzag	16.27	MD [30]
Peptide NT	–		MD [31]
C, BN	Zigzag	28.19	MD [32]
C	Armchair	**142.4***	MD [17]
WS_2	Zigzag, armchair	**195.5**	MM [16]

Note. * — multiwall nanotube, diameter is specified for external component. If asterisk is absent, the diameter is for single wall nanotube (SWNT).

The inorganic nanotubes based on WS_2 and oxides of transition metals attracted significant attention of researches due to their electronic, structural and mechanical properties. This fact means importance of *ab initio* modeling of such nanotubes using density functional theory (DFT).

Diameter of experimentally synthesized nanotubes ($\sim 2-300$ nm) in major cases is much higher the diameter of modeled nanotubes. This may lead to discrepancies between theoretical and experimental data, especially for mechanical and electronic properties. Maximum diameter of modeled inorganic nanotubes was 195.2 Å (MD), at that NT was achiral (zigzag) [16].

Authors of papers [34,35] showed that diameter and ration of indices of chirality n_2/n_1 of nanotubes can be experimentally measured with high accuracy. Besides in paper [20] the chiral angles θ of single-wall components of multi-wall nanotubes were determined. In said paper the method of active synthesis of multi-wall nanotubes with chiral angle similar for single-wall components was suggested. As effective MD/MM modeling is possible for multi-wall nanotubes, which components have same chiral angles, this experimental approach is also important for theoretical studies of properties of multi-wall nanotubes.

Considering all the above, it is of utmost importance to understand how to effectively perform theoretical modeling of large diameter chiral nanotubes to establish agreement between theory and experiment.

We will focus on nanotubes WS_2, as this material demonstrates potential for photocatalytic splitting of water [11], this is important source of „green" hydrogen energy. Besides, *ab initio* modeling of such type nanotubes using the theory of line groups was already performed by our scientific group [25], so the suggested earlier approach will be developed in present paper.

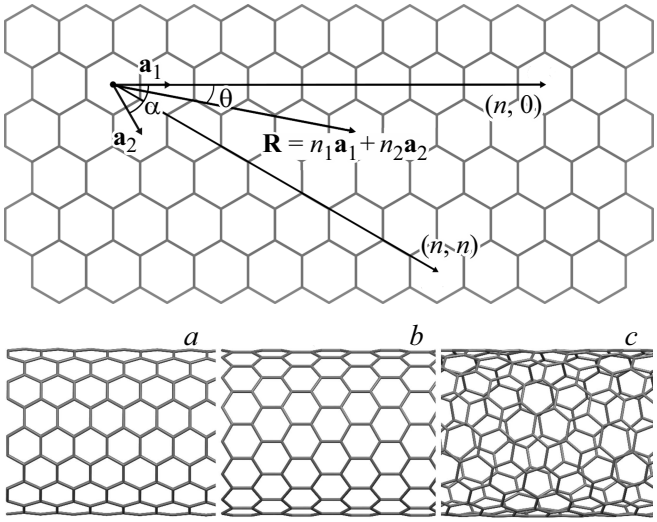

Figure 1. Hexagonal monolayer and rolled up from it nanotubes of different types: a — achiral „armchair" (n, n); b — achiral „zigzag" $(n, 0)$; c — chiral (n_1, n_2).

2. Symmetry of nanotubes rolled up from hexagonal layer

Let's review the hexagon layer with parameters $a = |\mathbf{a}_1| = |\mathbf{a}_2|$, angle between vectors of elementary translations $\alpha = 60°$. The chiral vector $\mathbf{R} = n_1\mathbf{a}_1 + n_2\mathbf{a}_2$ becomes the length of circle of nanotube during rolling up. Layer and appropriate nanotubes are shown in Figure 1.

Then diameter d can be calculated by formula

$$d = \frac{a}{\pi} n\sqrt{\tilde{n}_1^2 + \tilde{n}_1\tilde{n}_2 + \tilde{n}_2^2}, \tag{1}$$

where n — greatest common divisor (GCD) between (n_1, n_2).

Due to orthogonality condition $\mathbf{R} \cdot \mathbf{T} = 0$ ratio of components of translation vector $\mathbf{T} = t_1\mathbf{a}_1 + t_2\mathbf{a}_2$ is also determined by $\tilde{n}_1$ and $\tilde{n}_2$:

$$\frac{2\tilde{n}_1 + \tilde{n}_2}{\tilde{n}_1 + 2\tilde{n}_2} = -\frac{t_2}{t_1}. \tag{2}$$

Order of helical axis of NT is determined by formula (3)

$$q = n\tilde{q} = n\begin{vmatrix} \tilde{n}_1 & \tilde{n}_2 \\ t_1 & t_2 \end{vmatrix}. \tag{3}$$

Helical vector $\mathbf{H}$ is important characteristic of tubes helicity, and its uses are described in detail in review [14]. Components of helical vector determine number r of turns of rotation about axis of spiral with order $\tilde{q}$:

$$\tilde{n}_1 h_2 - \tilde{n}_2 h_1 = 1, \tag{4}$$

Table 2. Structural properties of NT with experimentally obtained chirality indices and diameters [35]

(n_1, n_2)	d_{exp}, Å	q	$N_{\text{at.}}(3 \cdot q)$	t, Å	θ°	r
(109, 29)	126.4	31766	95298	687.6	11.495	4373
(121, 30)	138.8	38342	115026	755.4	10.1815	1269
(134, 30)	151.7	22876	68628	412.6	9.891	9903
(147, 30)	164.5	5982	17949	99.5	9.111	1791
(159, 30)	176.4	20634	61902	320.0	8.492	4803

$$r = h_1 t_2 - h_2 t_1. \tag{5}$$

Inclination of vector R relative to a_1 determines the chiral angle θ. Common formula for this angle can be obtained from simple geometrical considerations

$$\theta = \text{arctg}\left(\frac{\tilde{n}_2 |\mathbf{a}_2| \sin\alpha}{\tilde{n}_1 |\mathbf{a}_1| + \tilde{n}_2 |\mathbf{a}_2| \cos\alpha}\right), \tag{6}$$

where α — angle between vectors of elementary translations. In case of hexagonal layer the formula (6) is converted as follows

$$\theta = \text{arctg}\left(\frac{\tilde{n}_2\sqrt{3}}{2\tilde{n}_1 + \tilde{n}_2}\right). \tag{7}$$

Authors of paper [35] provide the experimentally determined ratio of chirality indices n_2/n_1 and diameters of single-wall components of 5-wall nanotube WS_2. Based on formula (1) they suggested the chirality indices for five single-wall components of multi-wall nanotube. Using these indices we can calculate q, r, number of atoms in elementary cell $N_{\text{at.}}$ and length of the translation vector $|\mathbf{T}| = t$ for all single-wall components of nanotube. All these values are given in Table 2.

Large value of $N_{\text{at.}}$ in elementary cell of single wall nanotube can result in the idea that not only quantum-mechanical, but even MD/MM modeling of these systems is possible. However, it will be shown that this obstacle can be overcome using the theory of line groups.

Let's consider now several expressions from the theory of spiral groups needed for further analysis and development of our method. See details in papers [13,15,25]. The line groups describe the symmetry of quasi-1D systems in which periodicity along one direction is possible. These groups can be factorized as $L = ZP$, where Z — the group of generalized translations and P — the point symmetry group of the monomer. The spiral groups can be divided into 13 families depending on the symmetry operations in P and Z. The chiral nanotubes WS_2 relate to the first family (factor-group $P = C_n$), and „armchair" and „zigzag" — to 4 ($P = C_{nh}$) and 8 ($P = C_{nv}$) families, respectively. Elements of group Z can comprise point and translation parts: spiral axis of order Q $(C_Q|f)$, or sliding plane $(\sigma_v|f)$. As there are no crystallographic limitations on order of axes, Q can be any real number. If Q is rational, then we can write $Q = q/r = (\tilde{q}n)/r$. This variable determines the spiral angle of tube $\varphi = 2\pi/Q = 2\pi r/q = 2\pi r/(\tilde{q}n)$. The line group of chiral nanotube WS_2 can be written as $L = T_q^r C_n$ („polymer factorization"). The crystallographic notation $L = Lq_p$ can be determined using the transition formula

$$rp = lq + n, \tag{8}$$

$$r\tilde{p} = l\tilde{q} + 1. \tag{9}$$

3. Different approaches to modeling of hexagonal nanotubes with large diameter

3.1. Use of torsion angles to reduce number of atoms in elementary cell

In paper [25] the method is suggested based on variable Q use to study torsional deformations of NT. The torsion deformation of tube means the change of nanotube's spiral angle. Before deformation the nanotube has spiral angle $\varphi_0 = \frac{2\pi}{\tilde{Q}_0}$. The torsion angle is determined using the formula

$$\omega = \varphi_x - \varphi_0. \tag{10}$$

Then deformed nanotube has $\tilde{Q}_x = \frac{2\pi}{\varphi_x} = \frac{\tilde{q}_x}{r_x}$. Number of formula units in elementary cell of deformed nanotube is $n\tilde{q}_x$. So, the torsional deformations are associated with change in parameter $\tilde{Q}_0$.

Let's consider nanotube $(109, 29)$ with $\tilde{Q}_0 = \frac{31766}{4373} = 7.26412$. Using numerical search in definite range Q, we can determine the torsional angle $\omega = -0.00021$, this corresponds to $\tilde{Q}_x = 7.26415 = \frac{385}{53}$. This value is close to the initial $\tilde{Q}_0$, so changes in tube structure are negligible, but number of atoms in the elementary cell abruptly decreases: from 95298 to 1155. We can attempt to clarify this effect using number theory, in particular the theory of Diophantine approximations. In general, it states that any real number can be represented approximately by a rational number. Dirichlet [36] assumed that for any irrational number α there are infinitely many fractions $\frac{p}{q}$ such that

$$\left|\alpha - \frac{p}{q}\right| < \frac{1}{q^2}. \tag{11}$$

If we consider value $\tilde{Q}_0 = \frac{31766}{4373}$ as approximation of top boundary of some irrational number then value $\tilde{Q}_x = \frac{385}{53}$ can also approximate this irrational number, at that formula (11) is satisfied for $\tilde{Q}_x = \frac{p}{q}$ and $\alpha = \tilde{Q}_0$. Results of quantum-mechanical modeling of deformed (109, 29) nanotube are given in Sec. 5.

3.2. Chiral nanotube approximation by another chiral nanotube

Using formulas (2)−(5), we can determine that for second SW-component of 5-wall experimental nanotube from Table 2, (121, 30) $q = 8342$, $d = 138.8$ Å,

Table 3. results of numerical search of nanotubes with fixed q, equal to 182

(n_1, n_2)	d, Å	$\tilde{Q}$
(9, 1)	9.60	1.117
(16, 1)	16.62	1.065
(6, 5)	9.60	5.515
(11, 8)	16.62	2.716
(21, 7)	25.39	1.368
(35, 14)	43.97	2.364
(26, 13)	34.60	1.556
(52, 13)	59.92	1.273
(91, 0)	91.53	2.000
(91, 91)	158.64	2.000

$\theta = 10.815°$. Considering the nanotube with chirality parameters $(120, 30) = 30(4, 1)$, we can obtain the following values: $q = 420$, $d = 137.8$ Å, $\theta = 10.893°$. This nanotube, being similar to the experimental one $(121, 30)$, contains less atoms in elementary cell, 1260 instead of 115026.

Besides, using method suggested in Sec. 3.1, we can determine that for the torsion angle $\omega = -0.00006°$ we have $q = 423$. It will be shown that both approaches are applicable as we obtained similar results for both nanotubes.

3.3. Chiral nanotube approximation by achiral nanotube

It is known that for nanotubes the band gap and position of top of valence band and bottom of conduction band almost do not depend on chirality in case of large diameter. So, to study these properties the achiral tubes application is the best approach. For selected diameters $d = 126.4$ and $d = 138.8$ Å, using formula (1) we can determine achiral (n, n) and $(n, 0)$ nanotubes $(73, 73)$, $(126, 0)$, $(80, 80)$, $(138, 0)$. For the achiral nanotubes $q = 2n$.

Note that for one q we can obtain nanotube with different diameters, as chirality indices (n_1, n_2), q and d are interrelated by formulas (1)–(3). For example, at $q = 182$ one can obtain the following results (Table 3):

4. Method of quantum-chemical calculations

Ab initio calculations were performed in program CRYSTAL17 [37,38] using functional HSE06 (hybrid with 25% of Hartree-Fock exchange). The rationale for the choice of the basis set and the relativistic effective core pseudopotentials for W and S can be found in [25]. Splitting of Brillouin zone (BZ) to sections $18 \times 1 \times 1$ using Monkhorst–Pack grid was set [39], this gives in general 10 k-points, uniformly distributed over BZ. self-coupling was assumed as completed when difference of energies between two cycles was below 10^{-9} a.u. Criteria of calculation accuracy of Coulomb and exchange integrals were set at level 10^{-10} 10^{-10} 10^{-10} 10^{-10} 10^{-20} a.u. These criteria mean that during direct summation over grid the single electron integrals and two-electron Coulomb integrals below 10^{-10} are estimated using multipole expansion, and the two-electron exchange integrals are below 10^{-20} are ignored. Additional information can be found in User Manual CRYSTAL17 [40]. Geometry was optimized for both atomic coordinates and translation vector lengths. Threshold of the gradient was set equal to 0.001 a.u. Bohr^{-1}. Criterion of atomic convergence by atomic displacement was set equal to 0.005 Bohr.

5. Results and discussion

Besides two experimentally characterized in [35] single-wall nanotubes, (109, 29) and (121, 30), we present results of our method application to calculate several chiral nanotubes with diameter ~ 100 Å, which correspond to chiral angles obtained experimentally in [20]: $\theta = 2, 13, 15, 17°$. The nanotube formation energy (kJ/mol) is calculated by formula

$$E_{str} = \frac{E_{NT}}{N_{NT}} - \frac{E_{mono}}{N_{mono}}, \tag{12}$$

where number of formula units in the primitive cell for nanotube and monolayer is N_{NT} and N_{mono}, respectively. Full electron energies per primitive cell of nanotube and monolayer are presented E_{NT} and E_{mono}, respectively. Table 4 gives the results of quantum-mechanical modeling of different nanotubes with approximate diameter 126.4 Å.

It is evident that band gap of the nanotube with large diameter approaches value of layer (2.53 eV [25]) for both achiral, and chiral nanotubes. The optimized diameters correspond to experimental measured diameters of components of multi-wall nanotube. These results also indicate that deformation of the initial nanotube has negligible effect on its properties. But the larger angle ω is the larger are effect on the diameter and values of formation energy (see Appendix). Results of other calculations showed that angles $|\omega|$ over 0.004° result in increase in deformation energy to 100 kJ/mol and increase in diameter to 150 Å due to the rupture of the nanotube. Same effect is observed for polytwistane in paper [41] and requires additional studies. For further consideration see Table 5, providing results of calculation of nanotubes presenting experimental diameter 138.8 Å.

Note that for this diameter E_{str} of deformed nanotube hows minimum value as compared tochiral (120, 30) and achiral nanotubes. In this case, the value of the band gap is close to that for the monolayer (2.53 eV), and all optimized diameters coincide with the experimental results. Translation vectors for nanotubes (121, 30) and (109, 29) have same value $t = 8.36$ Å, though these nanotubes have different chiral angles: 10.8 and 11.5° respectively, and their initial translation vectors are different: 765.4 and 687.5 Å respectively. value 100 Å was given in [20] as minimum diameter of component of multi-wall nanotube. In this case

Table 4. Formation energies, optimized diameters, band gap and optimized translation vectors for nanotubes with diameter corresponding to (109, 29)

(n_1, n_2)	$\mathbf{L}q_p$	$\omega^{\circ *}$	$d_{\text{opt.}}$, Å	E_{str}, kJ/mol	E_{gap}, eV	t, Å
(109, 29)	$\mathbf{L}385_{247}$	−0.00021	126.9	1.22	2.529	**8.36**
(73, 73)	$\mathbf{L}146_{73}$	0	126.7	1.13	2.531	3.16
(126, 0)	$\mathbf{L}252_{126}$	0	126.9	1.16	2.531	5.47

Note. * — calculated by equation (10).

Table 5. Deformation energies, optimized diameters, band gap and translation vectors for different approaches to presentation of experimental diameter (121, 30) of nanotube

(n_1, n_2)	$\mathbf{L}q_p$	ω°	$d_{\text{opt.}}$, Å	E_{str}, kJ/mol	E_{gap}, eV	t, Å
(121, 30)	$\mathbf{L}423_{272}$	−0.00006	139.4	0.843	2.533	8.36
(120, 30)	$\mathbf{L}420_{270}$	0	138.4	0.953	2.532	8.36
(80, 80)	$\mathbf{L}160_{80}$	0	138.9	0.93	2.533	3.16
(138, 0)	$\mathbf{L}276_{138}$	0	138.4	1.02	2.533	5.47

Table 6. Formation energies, optimized diameters, band gap and optimized translation vectors for different chiral nanotubes with fixed diameter ∼ 100 Å

θ°	(n_1, n_2)	$\mathbf{L}q_p$	ω°	$D_{\text{opt.}}$, Å	E_{str}, kJ/mol	E_{gap}, eV	t, Å
2	(101, 4)	$\mathbf{L}206_{101}$	−0.001	103.8	3.63	2.513	5.47
13	(87, 27)	$\mathbf{L}315_{201}$	−0.010	103.9	4.26	2.504	8.36
15	(84, 31)	$\mathbf{L}314_{199}$	−0.002	103.8	11.06	2.432	8.37
17	(81, 35)	$\mathbf{L}313_{197}$	−0.003	104.0	22.19	2.318	8.39

the properties are more sensitive to chirality. Table 6 gives results of calculation of four chiral nanotubes WS_2.

All these nanotube have optimized diameters close to 104 Å, have small values E_{str} (about units and tens kJ/mol). As the diameter is smaller than in nanotubes (109, 29) and (121, 30), here it is possible to use larger torsional deformation. With increase in chiral angle we can see the decrease in band gap.

For the material to be suitable for photocatalytic water splitting, several requirements shall be met — the band gap values shall be in the visible range (1.5−2.6 eV), and energy of top of valence band E_{VB} and bottom of conduction band E_{CB} shall enter the range $E_{VB} < -5.67$ eV and $E_{CB} > -4.44$ eV (values of oxidation and reduction potentials of water). Besides, electronic transition $E_{CB} \rightarrow E_{VB}$ shall be straight, otherwise probability of recombination of charge carriers — electron/hole increases. The calculation results of these properties are presented in Table 7.

All considered nanotube, except (84, 31), comply with thew formal requirements of photocatalyst for water splitting. But values of band gap are getting very close to the border (2.6 eV), which from practical view can result in decrease in efficiency of this material as photocatalyst.

6. Conclusion

Methods *ab initio* of modeling hexagonal nanotubes of large diameter are presented and evaluated on the example of chiral nanotubes WS_2 with experimentally determined diameters and chiral angles. Obtained results indicate that the use of achiral „armchair" nanotubes is the most efficient approach to reduce the number of atoms in the elementary cell to match the desired diameter. If necessary in the specific situations other strategies can be used. Though the approach based on torsional deformation ensures making insignificant structural changes in nanotube, for example, reduce order of axis of rotation q and translation vector by several orders, it can be implemented under definite conditions only. In particular, this approach is effective for chiral nanotubes only, in which there is a possibility to decrease significantly the number of atoms in the elementary cell. Despite the evident limitation, exactly use of the torsional deformation ensures achievement of the experiment compliance with theoretical modeling. Achiral nanotube with large diameter can be modeled by general method, as they have large symmetry and low translation vector.

Table 7. Single-electron properties of modeled nanotubes WS_2

(n_1, n_2)	$\mathbf{L}q_p$	d_{opt}, Å	E_{VB}, eV	E_{CB}, eV	E_{gap}, eV	Type of transition
(109, 29)	$\mathbf{L}385_{247}$	126.9	−6.43	−3.91	2.595	Direct
(73, 73)	$\mathbf{L}146_{73}$	126.7	−6.46	−3.93	2.531	Direct
(126, 0)	$\mathbf{L}252_{126}$	126.9	−6.46	−3.93	2.531	Direct
(80, 80)	$\mathbf{L}160_{80}$	138.9	−6.45	−3.92	2.533	Direct
(138, 0)	$\mathbf{L}276_{138}$	138.4	−6.45	−3.92	2.533	Direct
(101, 4)	$\mathbf{L}206_{101}$	103.8	−6.46	−3.94	2.513	Direct
(87, 27)	$\mathbf{L}315_{201}$	103.9	−6.46	−3.96	2.504	Direct
(84, 31)	$\mathbf{L}314_{199}$	103.8	−6.45	−4.02	2.432	Indirect
(81, 35)	$\mathbf{L}313_{197}$	104.0	−6.43	−4.11	2.318	Direct

For chiral nanotubes low torsional deformations ensure modeling of the stable nanotubes. With increase in absolute value of torsion angle the deformation energy significantly increases, as well as the nanotube diameter. All modeled in this paper nanotubes, except one, in potential can be used as photocatalyst for the water splitting.

Acknowledgments

The authors highly appreciate the assistance of the „Computing Center of St. Petersburg State University“ in conducting high-performance computing.

Conflict of interest

The authors declare that they have no conflict of interest.

References

[1] S. Iijima. Nature **354**, *6348*, 56 (1991).
[2] R. Tenne, L. Margulis, M. Genut, G. Hodes. Nature **360**, *6403*, 444 (1992).
[3] A.P. Deshmukh, W. Zheng, C. Chuang, A.D. Bailey, J.A. Williams, E.M. Sletten, E.H. Egelman, J.R. Caram. Nature Chem. **16**, 800 (2024).
[4] A.A. Rajhi, S. Alamri. J. Mol. Mod. **28**, *2*, 50 (2022).
[5] M. Motamedi, E. Safdari. Silicon **14**, *10*, 5527 (2022).
[6] I.A. Bryukhanov, V.A. Gorodtsov, D.S. Lisovenko. Phys. Mesomech. **23**, *6*, 477 (2020).
[7] F. Najafi. J. Nanostruct. Chem. **10**, *3*, 227 (2020).
[8] D.L. Wilson, J. Ahlawat, M. Narayan. Explor. Neuroprotective Ther. 72, (2024).
[9] Q. Zhou, L. Zhu, C. Zheng, J. Wang. ACS Appl. Mater. Interfaces **13**, *34*, 41339 (2021).
[10] S. Ghosh, V. Brüser, I. Kaplan-Ashiri, R. Popovitz-Biro, S. Peglow, J.I. Martínez, J.A. Alonso, A. Zak. Appl. Phys. Rev. **7**, *4*, 041401 (2020).
[11] S. Piskunov, O. Lisovski, Y.F. Zhukovskii, P.N. D'yachkov, R.A. Evarestov, S. Kenmoe, E. Spohr. ACS Omega **4**, *1*, 1434 (2019).
[12] M. Damnjanović, B. Nikolić, I. Milošević. Phys. Rev. B **75**, *3*, 033403 (2007).
[13] M. Damnjanović, I. Milošević. Line groups in physics: theory and applications to nanotubes and polymers. Springer, Berlin Heidelberg (2010).
[14] E.B. Barros, A. Jorio, G.G. Samsonidze, R.B. Capaz, A.G. Souza Filho, J. Mendes Filho, G. Dresselhaus, M.S. Dresselhaus. Phys. Rep. **431**, *6*, 261 (2006).
[15] R.A. Evarestov. Theoretical Modeling of Inorganic Nanostructures: Symmetry and *ab initio* Calculations of Nanolayers, Nanotubes and Nanowires. Springer International Publishing, Cham. (2020).
[16] A.V. Bandura, S.I. Lukyanov, A.V. Domnin, D.D. Kuruch, R.A. Evarestov. Comput. Theor. Chem. **1229**, 114333 (2023).
[17] N.A. Sakharova, A.F.G. Pereira, J.M. Antunes, J.V. Fernandes. Materials **13**, *19*, 4283 (2020).
[18] Y. Rostamiyan, N. Shahab, C. Spitas, A. Hamed Mashhadzadeh. J. Mol. Mod. **28**, *10*, 300 (2022).
[19] M. Damnjanović, T. Vuković, I. Milošević. Isr. J. Chem. **57**, *6*, 450 (2017).
[20] Q. An, W. Xiong, F. Hu, Y. Yu, P. Lv, S. Hu, X. Gan, X. He, J. Zhao, S. Yuan. Nature. Mater. **23**, *3*, 347 (2024).
[21] P.N. D'yachkov. Quantum Chemistry of Nanotubes: Electronic Cylindrical Waves. CRC Press (2021).
[22] P.N. D'yachkov. ZhNKh **66**, *6*, 750 (2021). (in Russian).
[23] M.B. Sreedhara, Y. Miroshnikov, K. Zheng, L. Houben, S. Hettler, R. Arenal, I. Pinkas, S.S. Sinha, I.E. Castelli, R. Tenne. J. Am. Chem. Soc. **144**, *23*, 10530 (2022).
[24] L. Ju, P. Liu, Y. Yang, L. Shi, G. Yang, L. Sun. J. Energy Chem. **61**, 228 (2021).
[25] A.V. Domnin, I.E. Mikhailov, R.A. Evarestov. Nanomaterials **13**, *19*, 2699 (2023).
[26] A.V. Bandura, D.D. Kuruch, S.I. Lukyanov, R.A. Evarestov. Russ. J. Inorg. Chem. **67**, *12*, 2009 (2022).
[27] R.A. Evarestov, Yu.F. Zhukovskii, A.V. Bandura, S. Piskunov. J. Phys. Chem. C **114**, *49*, 21061 (2010).
[28] A. Evarestov, A.V. Bandura, V.V. Porsev, A.V. Kovalenko. J. Comput. Chem. **38**, *24*, 2088 (2017).
[29] S. Negi, M. Warrier, S. Chaturvedi, K. Nordlund. Comput. Mater. Sci. **44**, *3*, 979 (2009).
[30] Y. Wang, J. Zhao, Z. Tang. J. Mol. Liq. **393**, 123555 (2024).
[31] V. Bystrov, I. Likhachev, S. Filippov, E. Paramonova. Nanomaterials **13**, *13*, 1905 (2023).
[32] Q. Sun, J. Leng, T. Chang. Comput. Mater. Sci. **233**, 112725 (2024).
[33] H. Shin, E. Yeverovich, K.S. Kim. J. Mater. Res. **37**, *24*, 4483 (2022).
[34] H. Deniz, A. Derbakova, L.-C. Qin. Ultramicroscopy **111**, *1*, 66 (2010).
[35] Y. Chen, H. Deniz, L.-C. Qin. Nanoscale **9**, *21*, 7124 (2017).
[36] G.H. Hardy, E.M. Wright. An introduction to the theory of numbers. Oxford university press (1979).
[37] R. Dovesi, A. Erba, R. Orlando, C.M. Zicovich-Wilson, B. Civalleri, L. Maschio, M. Rérat, S. Casassa, J. Baima, S. Salustro, B. Kirtman. WIREs Comput. Mol. Sci. **8**, *4*, e1360 (2018).
[38] R. Dovesi, F. Pascale, B. Civalleri, K. Doll, N.M. Harrison, I. Bush, P. D'arco, Y. Noël, M. Rérat, P. Carbonnière. J. Chem. Phys. **152**, 20 (2020).
[39] H.J. Monkhorst, J.D. Pack. Phys. Rev. B **13**, *12*, 5188 (1976).
[40] R. Dovesi, V.R. Saunders, C. Roetti, R. Orlando, C.M. Zicovich-Wilson, F. Pascale, B. Civalleri, K. Doll, N.M. Harrison, I.J. Bush. https://www.crystal.unito.it (2017).
[41] A.V. Domnin, V.V. Porsev, R.A. Evarestov. Comput. Mater. Sci. **214**, 111704 (2022).

Translated by I.Mazurov